scientific reports

OPEN

Hybrid optimization for DC resistivity imaging via intelligible-in-time logic and the interior point method

Paul Edigbue✉, Hammed Oyekan, Abdullatif Al-Shuhail & Sherif Hanafy

Geophysical DC resistivity imaging is crucial in subsurface exploration, environmental studies, and resource assessment. However, traditional inversion techniques face challenges in accurately resolving complex subsurface features because of the inherent nonlinearities in geophysical data. To overcome these challenges, we propose a hybrid optimization approach that combines incomprehensible but intelligible-in-time (IbI) logic with the interior point method (IPM). The IbI logic framework leverages complexity and temporal intelligibility, allowing for a dynamic interpretation of subsurface phenomena. By integrating IbI with IPM, our approach benefits from global exploration and local refinement, leading to improved convergence speed and solution quality. The objective function formulated for the inversion process includes data misfit and model regularization terms, which promote accurate and smooth solutions. Our methodology involves the use of the IbI logic algorithm (ILA) for initial global search, which identifies promising regions in the search space. This is followed by the application of IPM for local optimization. This synergy between the two algorithms ensures robustness and efficiency in handling large datasets and complex geological models. We conducted tests using synthetic and real DC resistivity data to validate our approach. The synthetic test demonstrated the accurate reconstruction of subsurface anomalies, whereas the real data test successfully identified fault zones, which is consistent with previous studies. The hybrid optimization algorithm significantly improves the resolution of subsurface structures and enhances geophysical data inversion practices. It balances the exploration and refinement phases effectively, optimizing the computation time and ensuring precise model delineation.

Keywords Geophysical inversion, DC resistivity imaging, Hybrid optimization, IbI logic algorithm, Interior point method

Geophysical methods, especially DC resistivity imaging, are crucial in subsurface exploration, environmental studies, and resource assessment. The inversion of DC resistivity data is a fundamental process that aims to reconstruct the subsurface resistivity distribution from measured data, providing valuable insights into geological structures and hydrogeological properties[1,2]. Traditional inversion techniques, such as least-squares methods and linearized inversion algorithms, have been widely used to address these problems. These methods often face challenges in accurately resolving complex subsurface features and handling the nonlinearities inherent in geophysical data[3,4].

To address these challenges, various advanced optimization algorithms have been developed. For example, evolutionary algorithms such as genetic algorithms and particle swarm optimization have been employed to improve inversion resolution by effectively exploring the global search space. These algorithms have demonstrated significant improvements in overcoming local minima and enhancing convergence speed[5,6]. However, these methods still have limitations, such as insufficient adaptability to complex geological structures and computational inefficiency when handling large datasets. The need for more robust and efficient inversion methods has led to the exploration of hybrid optimization approaches, which combine the strengths of multiple algorithms to increase performance[6,7]. In this context, we propose a novel hybrid optimization algorithm that integrates Intelligible-in-time (IbI) logic with the interior point method (IPM).

The IbI logic framework leverages complexity and temporal intelligibility, allowing for a dynamic interpretation of subsurface phenomena[8]. This technique offers a novel approach for interpreting DC resistivity

King Fahd University of Petroleum & Minerals, Dhahran, Saudi Arabia. ✉email: paulirikefe.edigbue@kfupm.edu.sa

data, particularly in areas with diverse subsurface characteristics. By acknowledging the incomprehensible aspects of specific geological processes and the constraints of conventional linear models, IbI establishes a structure for capturing the dynamic and evolving nature of subsurface formations[9]. The fundamental concept of applying IbI in geophysics involves embracing uncertainty and nondeterminism as inherent traits of the Earth's subsurface. Instead of pursuing definitive solutions or exact forecasts, IbI encourages the investigation of the developing patterns and trends in geophysical data, facilitating a better understanding of intricate geological systems[10]. Implementing IbI leads to the adoption of adaptive approaches that evolve over time, responding to new data insights and emerging patterns. This dynamic data interpretation and modeling method enables a more significant understanding of subsurface processes, resulting in enhanced predictions and interpretations in geophysical investigations.

The interior point method (IPM) is a highly effective optimization technique widely utilized in various fields, such as geophysics, to address intricate inverse problems and optimization challenges[11]. Specifically, in geophysics, IPM is a reliable framework for effectively resolving extensive inverse problems associated with subsurface characterization, imaging, and parameter estimation[11,12]. The fundamental concept behind the interior point method centers on its capacity to navigate within the feasible region of a convex optimization problem by progressively advancing toward the interior of the possible set while satisfying the constraints. This approach enables the proficient resolution of optimization problems featuring many variables and constraints, making it particularly well suited for geophysical applications that involve high-dimensional data and complex geological structures. Furthermore, the interior point method offers scalability and computational efficiency advantages, making it suitable for handling large datasets and complex geological models encountered in geophysical studies[12]. By integrating IbI with IPM, our approach benefits from global exploration and local refinement, leading to improved convergence speed and solution quality.

This study focuses on developing a comprehensive framework for integrating hybrid optimization techniques into the inversion of geophysical DC resistivity data. By formulating an objective function that captures the misfit between observed and predicted data while incorporating logic-based constraints derived from geological knowledge, the proposed approach aims to improve the resolution of subsurface structures and enhance the characterization of geological features.

Through test examples and an analysis of inversion results, this study seeks to demonstrate the effectiveness and potential of the hybrid optimization approach in enhancing the inversion of DC resistivity data. These findings are relevant for advancing the field of geophysical data inversion and provide valuable insights for improving subsurface imaging techniques in geophysics and related disciplines.

Methodology

Hybrid optimization approach

Our novel approach combines the population-based metaheuristic IbI logic algorithm (ILA) with the interior point method (IPM) to address optimization problems. By combining the global search capabilities of the ILA with the local optimization efficiency of the IPM, we can effectively and efficiently solve the optimization problem. This process offers a novel opportunity to apply the ILA and IPM algorithms to solve an inversion optimization problem involving DC resistivity data. First, we utilize ILA to explore the search space systematically and generate diverse initial solutions for the inversion problem. Through innovative IBI logic theory-based strategies, the ILA quickly identifies promising regions of the search space without explicit knowledge of the problem structure. Subsequently, we employ the local optimization power of IPM to refine the solutions obtained from the ILA, ensuring accuracy while adhering to defined constraints. The best solutions from the ILA exploitation phase act as initial guesses for the IPM algorithm, facilitating further refinement. One drawback of local optimization algorithms is that they require reasonable starting solutions to achieve a high chance of success and prevent trapping in local minima. For this reason, we deployed the interior-point local search algorithm at the end of the ILA global search (Fig. 1). The synergy between ILA and IPM creates a feedback loop that enhances the optimization process by combining global exploration and local refinement, ultimately leading to improved convergence and solution quality.

The parameters determined by the ILA serve as an initial model for the IPM. The ILA generates an initial estimate of the subsurface resistivity distribution by leveraging its ability to interpret and integrate temporal and spatial data intelligibly. This initial model provides a starting point for the IPM, ensuring that the subsequent optimization process begins with a solution that is already closely aligned with the underlying geological structures. By starting from a more accurate initial model, the IPM can achieve faster convergence and improved solution quality. During the iterative process of the IPM, the parameters derived from the ILA are also used as a reference model. This reference model serves as a guide to ensure that the IPM maintains adherence to the geological constraints and complexity captured by the ILA. Specifically, the reference model influences the objective function by introducing additional terms that penalize deviations from the ILA-derived model. This integration helps the IPM refine the solution iteratively, balancing the minimization of the data misfit with the preservation of the geological plausibility provided by the ILA. Therefore, the ILA primarily drives the hybrid approach, and IPM is only applied at the end of the global search to refine these solutions and improve the model.

Formulation of the objective function and constraints

The main aim of every optimization algorithm is to search for an optimal solution to a given problem according to a set of constraints, typically by minimizing or maximizing the cost or objective function. This makes it a fundamental aspect of an optimization problem, significantly influencing the quest for an optimal solution. As a result, we establish our objective function by contrasting the theoretical data with the actual field observations or measured data. This process includes evaluating the L2 norms of the error related to the variance between field observations and theoretical data. Notably, the objective function assigns weights to accommodate outliers

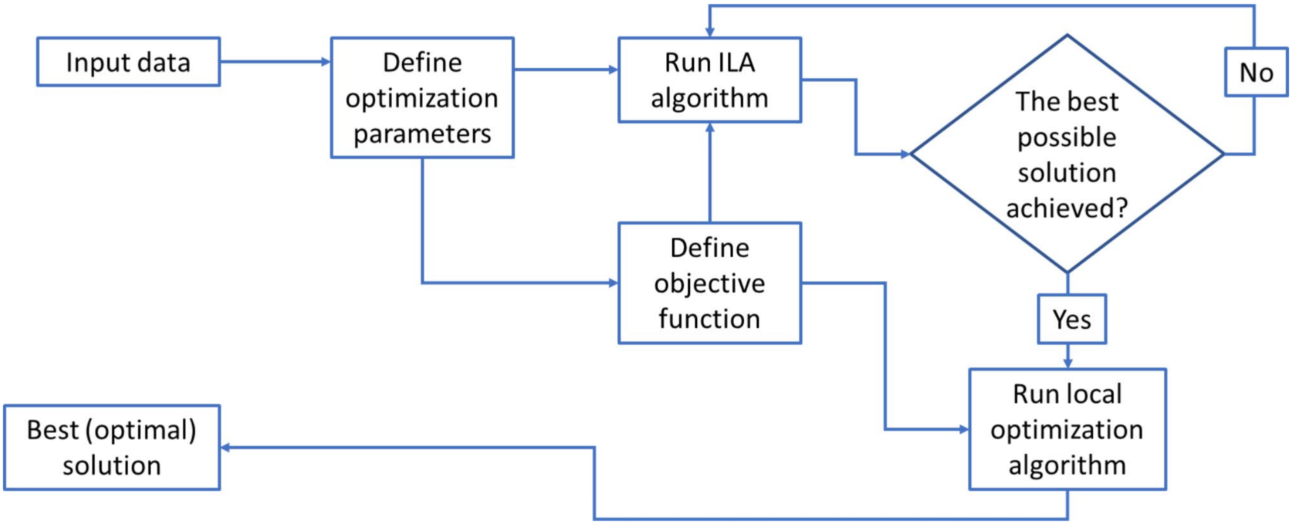

Fig. 1. Flowchart describing the hybrid optimization setup.

or erroneous observations. The objective function used in our inversion problem is composed of two terms: a data misfit, which is a normalized difference between observed and modeled data, weighted by $\boldsymbol{W_d}$, and a regularization term called the model misfit, which is proportional to the norm of the inverse of the variance of model parameters ($\boldsymbol{\sigma}$), scaled by a regularization parameter ($\boldsymbol{\lambda_{fm}}$). It penalizes significant variations in the model parameters to ensure smoothness. Consequently, the objective function is formulated as:

$$M_{dcr}(p) = misfit_{data}(p) + misfit_{model}(p) \tag{1}$$

$$M_{dcr}(p) = \frac{100.\|W_d.(d_{model}(p) - d_{obs})\|_2}{\|d_{model}(p)\|_2} + \lambda_{fm}.\|\frac{1}{\sigma}.\|_2 \tag{2}$$

$$W_d = \frac{1}{abs\left(d_{model(p)}\right) * 0.025} \tag{3}$$

where $\boldsymbol{M_{dcr}(p)}$ is the objective function relative to the DC resistivity method. $\boldsymbol{p}$ represents the vector of the resistivity model parameters. $\boldsymbol{W_d}$ is the data weighting matrix, $\boldsymbol{d_{obs}}$ represents the field-observed or field-measured data, and $\boldsymbol{d_{model}}(\boldsymbol{p})$ represents the modeled resistivity data obtained by solving the forward problem with parameter $\boldsymbol{p}$. The parameter 0.025 in Eq. 3 represents a scaling factor that balances the weight allocated to each data point owing to probable inconsistencies between the field-observed and theoretical data. The parameter λ balances the trade-off between data misfit and model regularization, preventing overfitting of the data and ensuring model stability in the inversion results. Through extensive testing on various synthetic and field datasets, optimal values for these parameters were obtained. These values were found to consistently yield optimal results in terms of convergence and accuracy.

Details of the inversion algorithm and parameter settings

Incomprehensible but intelligible-in-time logics algorithm (ILA)

Global ILA is intended to address complex problems by understanding how logic changes over time due to learning and experience (knowledge). This algorithm aims to find a nonlogic from a set of nonlogics that are likely to become a logic (general or special) of the future[8]. To achieve this, the process involves three stages, excluding an initial data preparation phase, which sets the foundation for the entire iterative optimization process by defining some conditions or properties that guide the algorithm's evolution. This phase creates clusters and assigns all the nonlogics (also referred to as populations or experts) specified by the user on the basis of the problem into groups via k-means clustering with the squared Euclidean distance (Eq. 4) as a distance metric to minimize within-cluster variance[8].

$$SED = d(x, y) = \sum_{i=1}^{n_{NL}} (x_i - y_i)^2 \tag{4}$$

The number of attempts (t_m) that the experts in a cluster make to enhance their initial nonlogic for each of the specified models is also determined at this stage. This calculation can be performed via

$$t_m = \frac{n_{t1}}{n_m} = \frac{p_{s1} N_T}{n_m} \tag{5}$$

where n_m is the number of models and where n_{t1} is the number of iterations for the exploration phase (stage 1), which is the product of the maximum percentage of iterations in stage 1 (p_{s1}) and the total number of iterations (N_T). The parameters are specified on the basis of the nature of the problem. Therefore, an appropriate selection of these parameters can increase the algorithm's efficiency. The algorithm's three main phases are the group work, integration, and exploitation or IbI logic search stages. The exploration phase is responsible for finding the best solutions in each available cluster in the global search space. It leverages the collective expertise of various "experts" or initial solutions. The best solutions from each cluster during the exploration stage are combined into a single group, and their NL values are updated on the basis of the available knowledge to refine and improve the quality of the solutions. This serves as the foundation for the integration phase. This phase of the algorithm aims to leverage the strengths of different experts (or solutions) to produce more comprehensive and robust solutions. Mirrashid and Naderpour 2023[8] thoroughly explained how to calculate the best solutions, update, and improve the knowledge of the combined experts at this stage. The exploitation phase produces the final optimized solutions in the search space. These solutions reflect the culmination of the iterative refinement and optimization process guided by the IbI framework. Each phase builds on the previous phase, ensuring a forward-moving progression where solutions in each phase move to the subsequent phase without returning to earlier phases after completion. The structured progression from broad exploration to detailed refinement and final optimization ensures that the algorithm effectively and continuously identifies and optimizes solutions over time.

The interior point method (IPM)

The interior point method (IPM) is a widely used algorithm in optimization, especially when dealing with problems with constraints such as variable bounds. The mathematical derivation of the IPM process is presented in[12] and[13]. However, we outline the overview of the IPM algorithm in Table 1, which provides a step-by-step guide on how the algorithm works. Let us examine the scenario where we aim to minimize a function $f(x)$ subject to constraints on the variables x, both upper and lower bounds. Mathematically, this can be expressed as:

$$min_x f(x) \tag{6}$$

subject to:

$$l \leq x \leq u, x \in \mathbb{R}^n \tag{7}$$

Here, x belongs to the set of real numbers $\mathbb{R}^n$, and l and u are vectors that represent the lower and upper bounds of the variables, respectively. The IPM operates by progressively enhancing a viable solution inside the feasible region defined by the constraints. The fundamental idea is to avoid boundaries at first and steadily converge toward the optimal solution by traversing through the interior of the feasible region[12].

To address the limitations imposed by the constraints $l \leq x \leq u$, an interior point method (IPM) employs a barrier function that penalizes the objective function as the solution approaches the boundary of the feasible region[13]. A commonly used barrier function is the logarithmic barrier, denoted as $\Phi(x)$, which is defined as the negative sum of the natural logarithms of the differences between the upper and lower bounds and the corresponding variables:

$$\Phi(x) = -\sum\nolimits_{i=1}^{n} \left(\ln(x_i - l_i) + \ln(u_i - x_i)\right) \tag{8}$$

Combining the objective function and the barrier function transforms the constrained optimization problem into a sequence of unconstrained problems. This is achieved by introducing a barrier parameter $\mu > 0$. The

IPM algorithm outline		
Step	**Description**	**Equation**
Initialization	Choose an initial barrier parameter μ_0. Define the convergence tolerance ε. Set $k = 0$	Let x_0 be an initial point such that $l < x_0 < u$
Iterative loop	For each iteration k: Define the Objective Function with Barrier Term:	$F_k(x) = f(x) + \frac{1}{\mu_k}\left(-\sum_{i=1}^{n}\left(\ln(x_i - l_i) + \ln(u_i - x_i)\right)\right)$ where $f(x)$ is the objective function term
	Calculate the Gradient $g_k(x)$:	$g_k(x) = \nabla f(x) - \frac{1}{\mu_k}\left(\frac{1}{x-l} - \frac{1}{u-x}\right)$
	Compute the Hessian $H_k(x)$:	$H_k(x) = \nabla^2 f(x) + \frac{1}{\mu_k} diag\left(\frac{1}{(x-l)^2} + \frac{1}{(u-x)^2}\right)$
	Solve for Newton Direction Δx_k:	$H_k(x_k)\Delta x_k = -g_k(x_k)$
	Update the Solution x: Update the Barrier Parameter μ:	$x_{k+1} = x_k + \alpha_k \Delta x_k$ $\mu_{k+1} = \beta \mu_k$
Check for convergence	If: $\left\| g_{k+1}(x_{k+1}) \right\| < \varepsilon$ then stop	Otherwise, set $k = k + 1$ and repeat the iteration steps

Table 1. Overview of the interior-point optimization algorithm.

parameter μ controls the barrier term in the IPM and is adaptively reduced during optimization. Its initial value and reduction schedule are selected on the basis of empirical validation to ensure fast convergence and accurate solutions. The barrier problem can then be formulated as minimizing the sum of the objective function $f\left(x\right)$ and the barrier function $\mu\Phi\left(x\right)$:

$$min_x\left(f\left(x\right)+\frac{1}{\mu}\Phi\left(x\right)\right) \tag{9}$$

The parameters used for the ILA and IPM algorithms are shown in Table 2. Fifty experts are considered, for which the number of iterations for each model is approximately 80, as given by Eq. 3. The greater the number of models selected, the lower the number of times the parameters of each model can be iteratively adjusted, which can potentially influence exploration, convergence, and the computational cost of finding optimal solutions. We allocate 33% of the total iterations (100) to the exploration phase of the global algorithm to ensure a comprehensive solution for space exploration. This helps to facilitate better initialization for the subsequent phases while still allowing ample resources for the integration and IbI logic search stages, promoting a balanced approach to optimization across all phases of the algorithm. We set the maximum number of iterations for finding the minimum in the IPM to 100. In contrast, the maximum number of objective function evaluations that the optimization solver can perform during local optimization is set to 100 times the dimensionality of the optimization problem (number of resistivity model parameters). In the context of our inversion problem, this is essentially the length of the parameter vector that the optimization algorithm adjusts to fit the observed resistivity data. The values of the parameters shown in Table 2 were determined on the basis of a combination of empirical testing, cross-validation, and sensitivity analysis to ensure optimal performance for our specific application. Each parameter was carefully chosen to balance the trade-off between convergence speed and inversion accuracy.

Test examples

In the hybrid optimization process, visualizing convergence plots offers valuable insights into the contributions made by the ILA algorithm. These contributions are shown through a convergence profile, which visually represents the distribution of contributions from the three phases within the ILA algorithm. The convergence profile illustrates the relationships among the contributions, fitness values, and number of iterations. By analyzing this chart, we gain a deeper understanding of the optimization progress at different stages of the ILA algorithm. This information helps identify patterns or trends that emerge during the optimization process. Once the best model is obtained through the ILA algorithm, it is passed on to local search techniques that employ the IPM algorithm. The results of this local search are then depicted in terms of minimizing fitness values over iterations. This allows for a more detailed analysis of the optimization progress and the effectiveness of the IPM algorithm in further improving the model. The optimal model is finally visualized as a 2D image plot to facilitate thorough analysis and interpretation. This plot provides a visual representation of the model, allowing objective examination of its characteristics and making informed decisions on the basis of the analysis.

Synthetic test

To evaluate the effectiveness of the proposed hybrid optimization algorithm, we created two synthetic 2D resistivity models that encompass two positive and two negative anomalies (Fig. 2). These synthetic models span a length of 240 m and a depth of 50 m, with the anomalies deliberately positioned near the center of the models. For the positive anomaly model, the background resistivity is set at 50 Ω-m, and each anomaly, which measures 30 m by 15 m, has a resistivity of 250 Ω-m (Fig. 2a). Similarly, for the negative anomaly model, the background resistivity is set at 250 Ω-m, and each anomaly, measuring 30 m by 15 m, has a resistivity of 50 Ω-m (Fig. 2b). To conduct the experiment, we used 49 electrodes with a 5-m spacing, utilizing the dipole−dipole array configuration for data acquisition. The resulting synthetic data were subsequently processed and presented in Res2DInv format with the addition of 30% Gaussian noise, ensuring its readiness for the inversion process. Specifically, 30% Gaussian noise of the maximum amplitude was added to the synthetic data, ensuring that the noise level was proportional to the signal strength and more representative of realistic scenarios.

The results of inverting the synthetic DC resistivity data via the hybrid optimization approach, beginning with the ILA algorithm, are presented in Figs. 3 and 4 for the positive and negative anomaly models, respectively.

Parameters	Value
Number of nonlogics (experts)$\left(n_{NL}\right)$	50
No of iterations $\left(\boldsymbol{N_T}\right)$ for IBI algorithm	100
No of models $\left(\boldsymbol{n_m}\right)$ required for the (IBI)	10
Percentage of Iteration in Phase 1 $\left(\boldsymbol{p_{s1}}\right)$	33%
Percentage of Iteration in Phase 2 $\left(\boldsymbol{p_{s2}}\right)$	33%
Maximum Iterations Allowed for Local Optimization $\left(\boldsymbol{MaxIter}\right)$	100
The number of function evaluations allowed for the local optimization,$\left(\boldsymbol{MaxFun}\right)$	100 * No of model parameters

Table 2. Parameters used in the hybrid optimization.

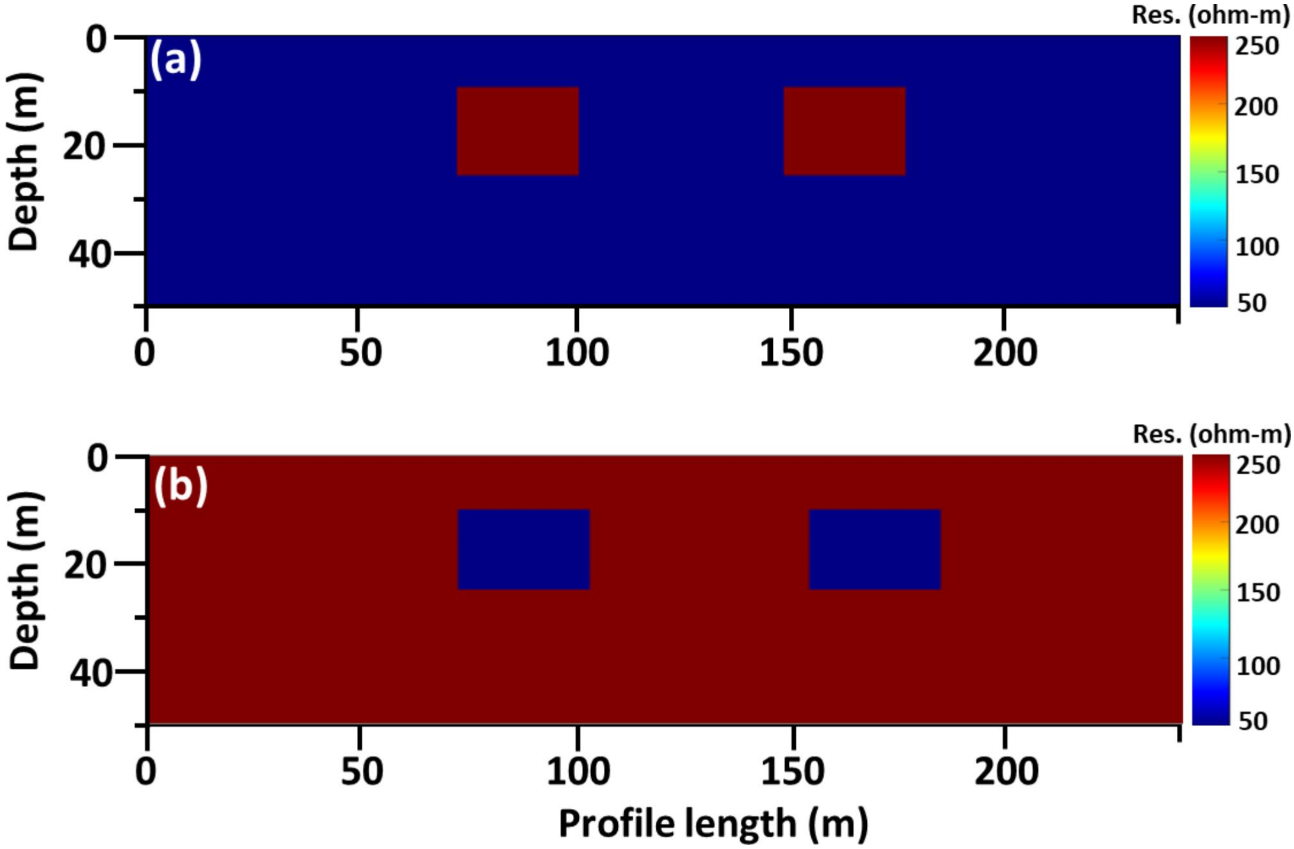

Fig. 2. Synthetic resistivity models showing pairs of (**a**) positive anomalies and (**b**) negative anomalies.

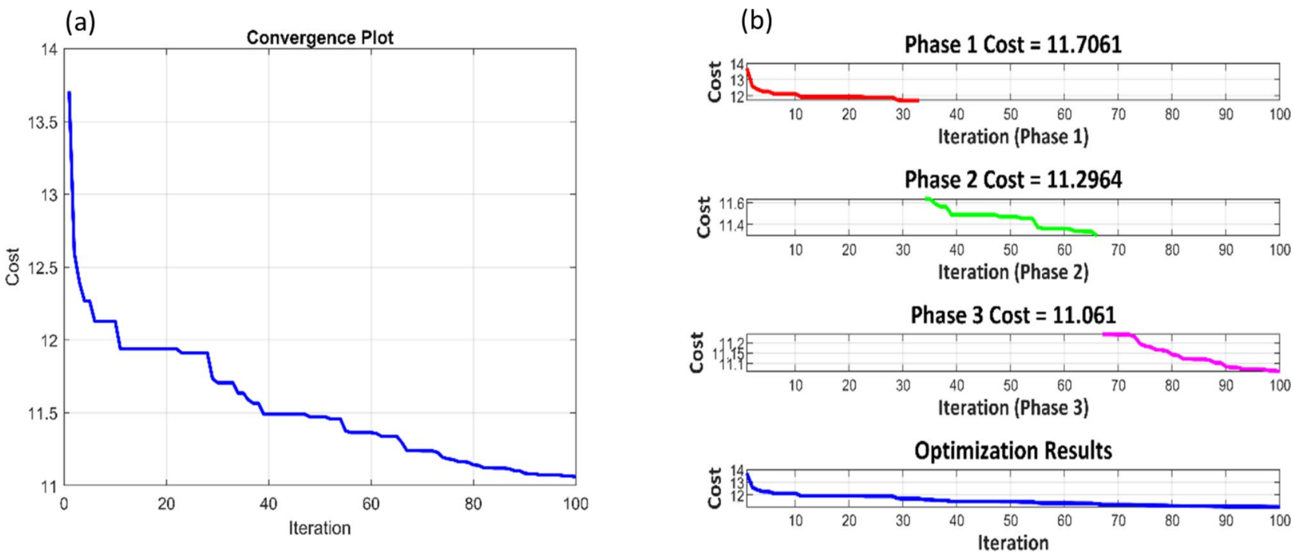

Fig. 3. Efficacy of the ILA optimization algorithm in DC resistivity data inversion for the positive anomaly model; (**a**) convergence plot showing cost function reduction over iterations and (**b**) contributions of each ILA phase to cost function minimization, highlighting their interdependence.

Figures 3a and 4a depict the algorithm's convergence over one hundred iterations, demonstrating how the algorithm iteratively reduces the misfit to achieve an optimal solution. Additionally, Figs. 3b and 4b illustrate the evolution of the misfit through the different phases of the ILA.

The hybrid optimization algorithm effectively reconstructs the geometry and amplitude of the resistive (positive anomalies) and conductive (negative anomalies) bodies in the synthetic models, as shown in Fig. 5a,b

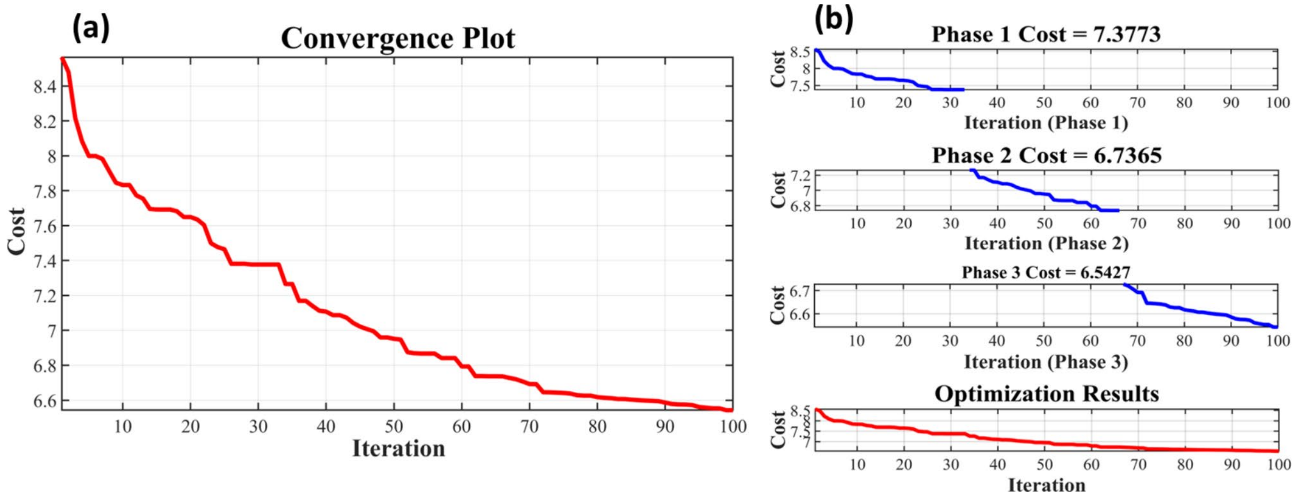

Fig. 4. Efficacy of the ILA optimization algorithm in DC resistivity data inversion for the negative anomaly model; (**a**) convergence plot showing cost function reduction over iterations and (**b**) contributions of each ILA phase to cost function minimization, highlighting their interdependence.

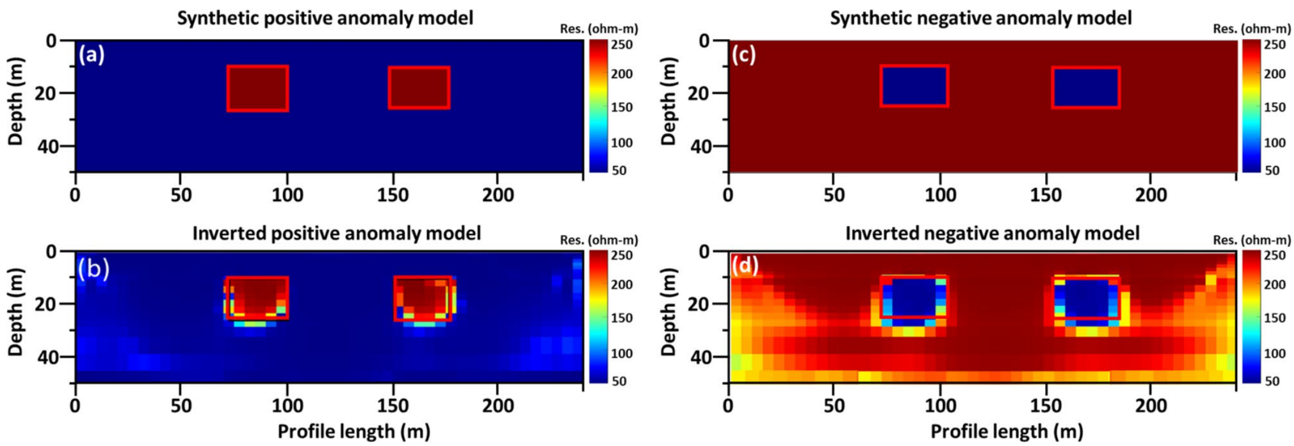

Fig. 5. Display and comparison of the (**a**) synthetic positive anomaly DC resistivity model, (**b**) positive anomaly inverted resistivity model, (**c**) synthetic negative anomaly DC resistivity model, and (**d**) negative anomaly inverted resistivity model.

for the positive anomalies and Fig. 5c,d for the negative anomalies. This demonstrates the algorithm's ability to accurately reconstruct subsurface structures. However, a minor discrepancy is observed in the spatial distributions of the anomalous bodies in the inverted models; they appear slightly diffuse compared with the well-defined anomalies in the synthetic models. This discrepancy is likely due to the high noise level added to the synthetic data and the approximation errors inherent in numerical modeling. Furthermore, the sensitivity of resistivity measurements decreases with depth, making accurate resolution of deeper structures more challenging, which is a common limitation in DC resistivity inversion.

Overall, the hybrid optimization algorithm, which combines the ILA with IPM techniques, shows better performance in reconstructing anomalies in terms of geometry and amplitude than do traditional optimization algorithms such as the Gauss-Newton and genetic algorithm approaches[6,14].

Real data test

The real resistivity data used in this study were acquired by[15] from an alluvial fan on the Gulf of Aqaba coast, as shown in the map produced using Google Earth imagery[16] in Fig. 6. Specifically, a 2D resistivity profile was obtained using 64 nodes with an electrode spacing of 5 m, employing a Schlumberger–Wenner array configuration, and spanning a total length of 315 m. Additional details regarding the data acquisition process, including the field layout and geometry, are provided in Hanafy et al.[15]. The 315 m-long acquisition profile cut across the location of an extensive surface rupture in the study area just south of Haql town caused by the Nuweiba earthquake of November 1995 within the alluvial deposits of the Saudi Arabian coast[15].

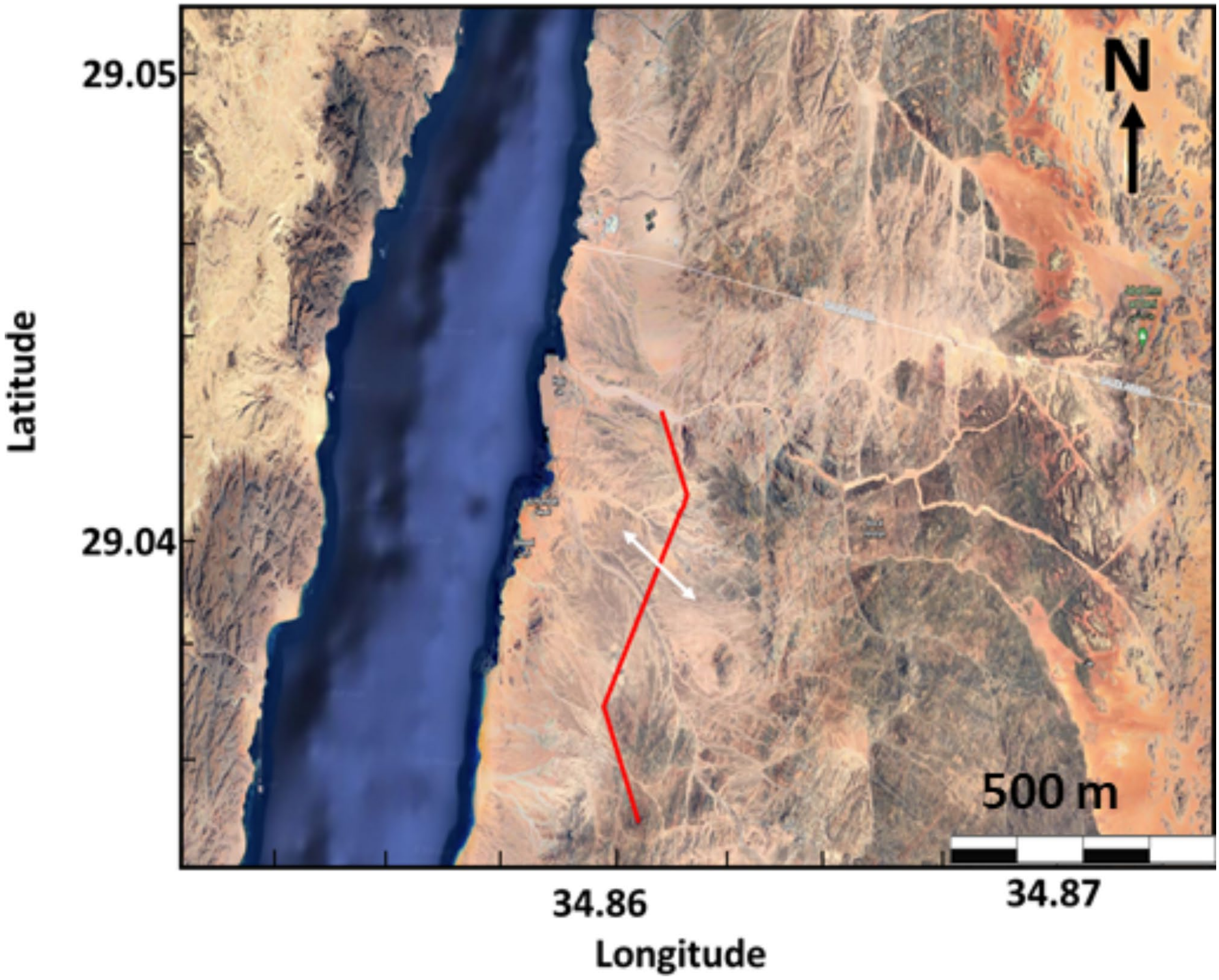

Fig. 6. The study area situated on the eastern side of the Gulf of Aqaba is depicted in a Google Earth satellite image[16]. The image shows the resistivity profile in white and visible normal faults highlighted in red. The map was generated using Google Earth Pro (version 7.3.6, available at https://www.google.com/earth/). The resistivity profile and fault lines were overlaid manually using the image annotation tools within Microsoft PowerPoint software.

For the adaptability of the proposed algorithm in DC resistivity inversion, we decided to use a portion of the data totaling a length of 200 m. This approach directly compares the resistivity data and the known location of the normal fault in the study area, ensuring accurate correlation and validation of the results. Additionally, this approach offers the opportunity to assess the effectiveness of the proposed algorithm in mapping subsurface features such as faults and fractures within alluvial sediment and enhancing model interpretation[15].

The inversion results obtained via the hybrid optimization algorithm are shown in Fig. 7, with the similar parameters listed in Table 2. Due to the challenging conditions of the real dataset, we initiated the hybrid algorithm with local optimization to refine the search space. This initial step was followed by global optimization to explore the broader solution space. Finally, the optimization process was completed using the local algorithm to achieve the best solution. As a result, the algorithm converged very quickly and was able to accurately reconstruct the subsurface resistivity distribution (Fig. 8).

Analysis of the accuracy and efficiency of the proposed approach

The proposed hybrid optimization approach was evaluated through test examples using synthetic data, real data applications, and statistical misfit analysis to determine its accuracy and efficiency. The results showed that the hybrid method excelled in reconstructing resistivity models, exhibiting significantly lower errors than the individual IbI logic and interior point methods did (Figs. 3, 4, 7). This was further supported by the alignment of the hybrid approach's models with geological expectations in real-world applications, providing additional evidence of its accuracy (Figs. 5, 8).

In terms of efficiency, the hybrid approach demonstrated faster convergence rates (44 min for the synthetic test and 21 min for the real data test) and maintained a balanced computational cost. This was achieved by leveraging

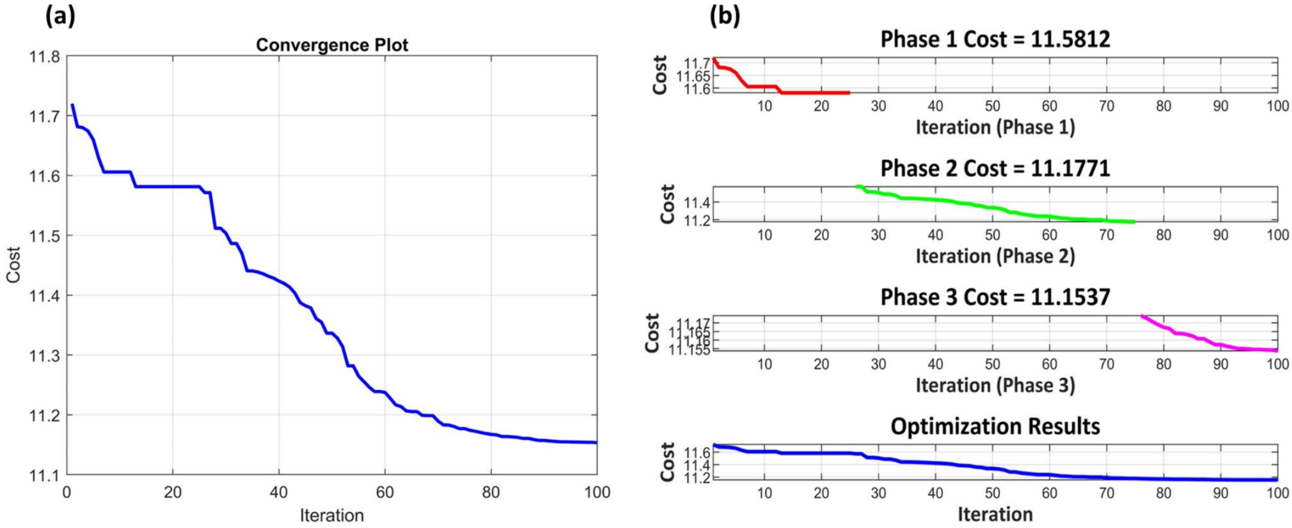

Fig. 7. Illustration of the inversion of real DC resistivity data, showing (**a**) the overall convergence plot of the algorithm and (**b**) phasewise convergence plots.

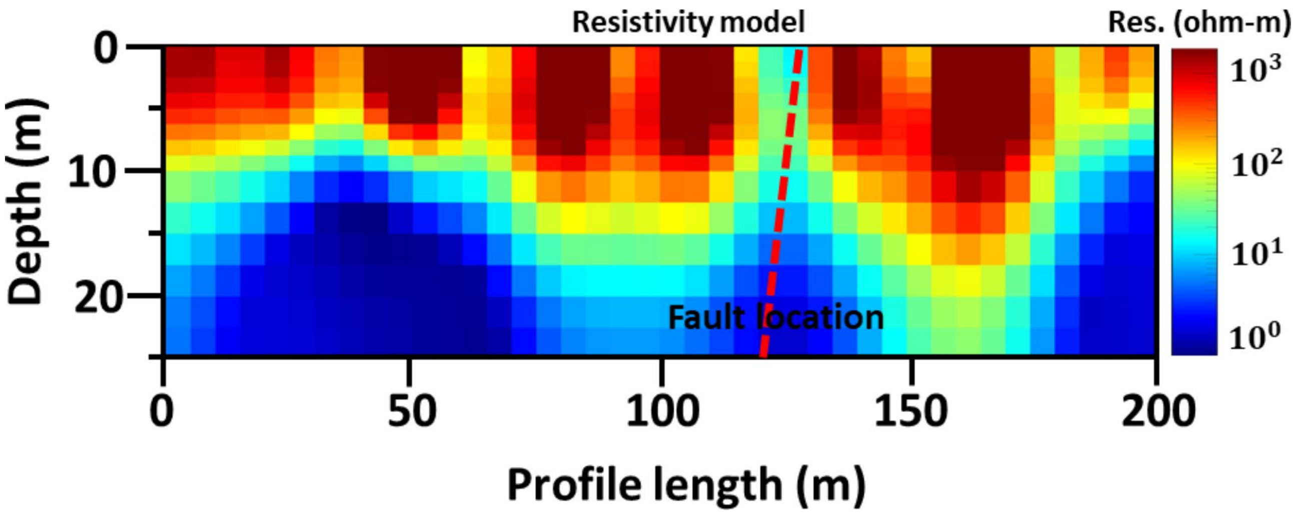

Fig. 8. The inverted resistivity model shows a significant anomalous discontinuity that is believed to indicate the presence of a fault (red dashed line). This observation is derived from the analysis of a real dataset.

the exploratory strength of the IbI logic and the local optimization capabilities of the interior point method. The hybrid method achieved quicker convergence while maintaining a feasible computational load, making it suitable for large-scale problems. Furthermore, scalability tests confirmed that the hybrid method retained its efficiency and accuracy advantages even when dealing with increasing problem sizes. This demonstrated the robustness and practicality of the hybrid approach for extensive geophysical inversion tasks.

Results and discussion

Interpretation of the results in the context of the research objectives

The resistivity model generated by the ILA algorithm does not exhibit distinct features; however, it effectively reduces the extensive search area to a more practical and plausible domain for the IPM algorithm. By refining the feasible search space, the ILA algorithm enhances the IPM and improves the overall efficiency of the hybrid optimization algorithm. This is evident in the optimal inverted resistivity models obtained from synthetic and actual data tests, demonstrating the ability of the algorithm to accurately delineate subsurface anomalies and discontinuities (Figs. 5, 8).

In terms of quantitative analysis, the comparison between the inverted resistivity model and the actual synthetic resistivity model revealed that the hybrid algorithm successfully reconstructed more than 90% of the resistivity anomaly. The reconstructed anomalies exhibited relatively similar geometric and resistivity values to those of the synthetic model, indicating the effectiveness of the algorithm in identifying subsurface discontinuities and anomalous features. Furthermore, in the inverted real data test, a significant anomalous discontinuity was observed at approximately 120 m along the profile length (Fig. 8). This finding aligns with previous studies conducted by[6] and[15], who utilized similar datasets in their respective research. These studies interpreted the observed anomalies as fault zones in relation to the ground observations within the study area.

Discussion of the advantages and limitations of the hybrid method

The hybrid optimization algorithm, which combines the ILA and IPM techniques, demonstrates not only its ability to accurately invert DC resistivity data but also its ability to optimize computation time. The synthetic test results in an average runtime of 44 min (100 nonlogics and 100 iterations), whereas the real data test results are only 21 min when the same parameters are used. The algorithm demonstrates promising performance with reasonable runtimes in both synthetic and real data tests. However, the differences in the inversion depth, survey length, and meshing must be considered when evaluating its overall feasibility and attractiveness for solving nonlinear DC resistivity inversion problems. While the hybrid algorithm effectively maps discontinuities and anomalies in the test examples, its robustness in more challenging geologic formations can be further validated with additional data from diverse geologic settings. Additionally, it is important to note that this algorithm requires a bounded constraint to define the search space. In situations where an inappropriate search is defined in the input parameter, the algorithm may fail to converge or become trapped in a local minimum of the fitness function. Therefore, it is recommended to establish lower and upper bounds for the search domain on the basis of a priori information.

Implications of the findings for geophysical data inversion practices

This study highlights the effective adaptation of a population-based optimization algorithm that can manage vast datasets and input variables to address geophysical optimization challenges. Notably, this population-based algorithm can be smoothly integrated with a conventional local search technique, as evidenced in this study. This fusion results in resilient hybrid optimization algorithms that capitalize on the unique strengths of each method. By utilizing a population-based algorithm that excels in handling extensive datasets, geophysical inversions can be more efficient, particularly when dealing with intricate models and large datasets. The incorporation of local search methods enables the fine-tuning of solutions obtained from population-based algorithms. This combined strategy ensures highly precise geophysical models that closely represent the underlying physical characteristics. The development and successful implementation of these hybrid optimization strategies significantly improve the feasibility and potential for the widespread adoption of geophysical inversion methods. Accurate and dependable geophysical models produced from robust inversion techniques ultimately contribute to effective and precise data interpretation endeavors, leading to a deeper comprehension of the subsurface properties under investigation.

Conclusion

This study introduces a new hybrid optimization strategy that combines incomprehensible but intelligent-in-time (IbI) logic with the interior point method (IPM) to increase the accuracy and efficiency of geophysical data inversion. The proposed method demonstrated satisfactory performance in both synthetic and real-world scenarios, producing resistivity models with reduced errors and better alignment with geological expectations. Misfit analysis and model comparison validated the precision of the hybrid approach, while its faster convergence rates and manageable computational load highlighted its efficiency.

This investigation makes a significant contribution to the field of geophysical data inversion by presenting a novel hybrid optimization technique that capitalizes on the advantages of global and local optimization methods. The integration of IbI logic and the interior point method overcomes the limitations of each technique, providing a robust solution for large-scale geophysical inversion tasks. This study offers a pragmatic and scalable approach, advancing the current methodologies for reconstructing resistivity models.

Subsequent studies should focus on exploring optimal strategies for integrating global and local optimization algorithms. Various methods for alternating between global IbI logic and local optimization procedures should be explored. Potential approaches involve transitioning on the basis of specific criteria, such as a decrease in misfit values after a set number of iterations or during periods of stagnation in the global optimization process. Through experimentation with these criteria, a more efficient hybrid algorithm can be developed, achieving faster convergence while maintaining reasonable computational efficiency. These advancements will further enhance the applicability and performance of hybrid optimization techniques in geophysical data inversion.

Data availability

The datasets utilized in the present research can be accessed through the KAUST repository at the following link: https://repository.kaust.edu.sa/items/421f1878-9025-495a-8981-880e50aad556.

Received: 17 June 2024; Accepted: 4 November 2024
Published online: 11 November 2024

References

1. Loke, M. H., Rucker, D. F., Chambers, J. E., Wilkinson, P. B. & Kuras, O. Electrical resistivity surveys and data interpretation. *Encyclopedia of Earth Sciences Series* https://doi.org/10.1007/978-3-030-10475-7_46-1 (2020).
2. Günther, T., Rücker, C. & Spitzer, K. Three-dimensional modelling and inversion of dc resistivity data incorporating topography—II. Inversion. *Geophys J Int* **166**, 506–517 (2006).
3. Edigbue, P. *et al.* Testing different stochastic methods to model direct current resistivity and seismic refraction geophysical data using a combined local and global optimization algorithm. *Arab J Sci Eng* **48** (2023).

4. Trainor-Guitton, W. & Hoversten, G. M. Stochastic inversion for electromagnetic geophysics: Practical challenges and improving convergence efficiency. *Geophysics* **76**, (2011).
5. Zhao, Z., Sen, M. K., Denel, B., Sun, D. & Williamson, P. A Hybrid optimization framework for seismic full waveform inversion. *J Geophys Res Solid Earth* **127** (2022).
6. Edigbue, P. *et al.* A comprehensive study of local, global, and combined optimization methods on synthetic seismic refraction and direct current resistivity data. *Applied Sciences (Switzerland)* **12** (2022).
7. Soupios, P., Akca, I., Mpogiatzis, P., Basokur, A. T. & Papazachos, C. Applications of hybrid genetic algorithms in seismic tomography. *J Appl Geophy* **75** (2011).
8. Mirrashid, M. & Naderpour, H. Incomprehensible but Intelligible-in-time logics: Theory and optimization algorithm. *Knowl Based Syst* **264** (2023).
9. Ma, Z., Kim, Y. Do, Volkov, O. & Durlofsky, L. J. Optimization of subsurface flow operations using a dynamic proxy strategy. *Math Geosci* **54** (2022).
10. Seyedan, M. & Mafakheri, F. Predictive big data analytics for supply chain demand forecasting: methods, applications, and research opportunities. *J Big Data* **7** (2020).
11. Li, Z., Yao, C., Zheng, Y., Wang, J. & Zhang, Y. 3D magnetic sparse inversion using an interior-point method. *Geophysics* **83** (2018).
12. Zhu, W. *et al.* Gravity sparse inversion using the interior-point method and a general model weighting function. *Studia Geophysica et Geodaetica* **64** (2020).
13. Ames, A. D. *et al.* Control barrier functions: Theory and applications. in *2019 18th European Control Conference, ECC 2019* (2019). https://doi.org/10.23919/ECC.2019.8796030.
14. Candansayar, M. E. Two-dimensional individual and joint inversion of three- and four-electrode array dc resistivity data. *Journal of Geophysics and Engineering* **5** (2008).
15. Hanafy, S. M., Jonsson, S. & Klinger, Y. Imaging normal faults in alluvial fans using geophysical techniques: Field example from the coast of gulf of aqaba, Saudi Arabia. In *Society of Exploration Geophysicists International Exposition and 84th Annual Meeting SEG 2014* (2014). https://doi.org/10.1190/segam2014-1007.1.
16. Google Earth. Google Earth [Version 7.3.4]. https://earth.google.com/ (2024).

Acknowledgements
The authors gratefully acknowledge CPG for their technical and financial support. Also, we acknowledge chatgpt and ahrefs, which were utilized to enhance readability and revise certain sections of the manuscript.

Author contributions
Conceptualization, method investigation, administration, and funding acquisition: P. E., A. A.; Methodology, investigation, and report writing: P.E., A. A., H. O.; Investigation, original draft preparation, review, and editing: P.E., A. A., H. O., S. H.

Funding
This research was funded by the start-up grant SF18060 from the College of Petroleum Engineering and Geosciences (CPG) at King Fahd University of Petroleum and Minerals (KFUPM).

Declarations

Competing interests
The authors declare no competing interests.

Additional information
Correspondence and requests for materials should be addressed to P.E.

Reprints and permissions information is available at www.nature.com/reprints.

Publisher's note Springer Nature remains neutral with regard to jurisdictional claims in published maps and institutional affiliations.